

## Sensitive and Selective Determination of Pb<sup>2+</sup> Ions Based on 2,5-Dimercapto-1,3,4-Thiadiazol Functionalized AlGa<sub>N</sub>/Ga<sub>N</sub> High Electron Mobility Transistor

This chapter reveals the development of the AlGa<sub>N</sub>/Ga<sub>N</sub> HEMT sensor to efficiently detect toxic lead (Pb<sup>2+</sup>) ions in the aqueous solution. In this chapter, the description contains the functionalization process of the AlGa<sub>N</sub>/Ga<sub>N</sub> HEMT using 2,5-di-mercapto-1,3,4, thiadiazol (DMTD) to detect Pb<sup>2+</sup> ions. The selectivity, repeatability, and other relevant analysis is explained in later sections.

### 6.1 INTRODUCTION

The pollution caused by heavy-metals ions to the environment is mainly due to mining, industrialization, and the chemicals produced by fertilizers and household waste, which is known to be a severe problem worldwide. The toxicity of heavy metals and their compounds are well known. These compounds readily enter into human and animal bodies by contaminating ecosystems, food-chain, and exposure to products that possess heavy metals [Chen *et al.*, 2018; Gumpu *et al.*, 2015]. Because of the hazardous nature of heavy metals, especially mercury (Hg), lead (Pb), and cadmium (Cd), the use of these metals is banned by the Restriction of the Use of Certain Hazardous Substances (RoHS) of the European Union in the Electrical and Electronic Equipment Directive [Shaily *et al.*, 2018]. Among many heavy metals, Pb is one of the most abundant and toxic elements. It is generally found in paints, batteries, building materials, industrial waste, sanitation PVC pipes, agricultural materials, petroleum products, packed food, rain, and lake water [Gumpu *et al.*, 2015; Swearingen *et al.*, 2005]. Excessive concentration of Pb increases the threat of serious health problems in humans and especially in children, such as neurodegenerative diseases, cardiovascular and developmental disorders, kidney damage, hyperirritability, decreased bone growth. Lead is a carcinogens element; it affects soft tissues and organs of the human body that leads to cancer; a higher concentration of Pb in the blood can cause coma and death [Chen *et al.*, 2018; Gumpu *et al.*, 2015; Shaily *et al.*, 2018; Swearingen *et al.*, 2005]. Due to the toxicity and hazardous nature of Pb, the maximum permissible limit of drinking water set by the World Health Organization (WHO) and Environmental Protection Agency (EPA) for Pb<sup>2+</sup> ions is 10 ppb and 15 ppb, respectively [Ariño *et al.*, 2017; Kumar *et al.*, 2017]. These reasons direct our attention and concern towards public health and require sensitive and selective detection of lead ions (Pb<sup>2+</sup>) at low concentrations.

The analytical methods such as spectrometry, fluorimetry, colorimetry, and electrochemical processes [Dong *et al.*, 2014; Vasimalai and John, 2011; Yang *et al.*, 2014; Zhu *et al.*, 2008] showed detection capabilities for Pb<sup>2+</sup> ions at trace levels. However, these are laboratory-based, time-consuming approaches with a lack of portability. Thus, it is necessary to develop a fast, real-time, user-friendly, and portable sensor for onsite, rapid, and accurate analysis of Pb<sup>2+</sup> ions in water.

Many approaches were employed for the development of portable Pb<sup>2+</sup> ion sensors like biofunctionalization, optical fiber-based, surface-enhanced Raman scattering (SERS), LC resonance, paper, and Si-field effect transistor-based [Shi *et al.*, 2018; Wang *et al.*, 2016; Xiao *et al.*, 2018; Yap *et al.*, 2018; Yeh and Yang, 2017; Zhang *et al.*, 2013; Zhou *et al.*, 2014]. Additionally, nanomaterials such as carbon nanotubes, gold, and silver nanoparticles (Au NP and Ag NP) are also utilized for the development of portable Pb<sup>2+</sup> ion sensors [Lou *et al.*, 2011; Shi *et al.*, 2018; Zhao *et al.*, 2014]. These methods showed an excellent response for Pb<sup>2+</sup> ion detection, but the inability of Si-based sensors in harsh environmental conditions and requirement of reference electrode provides direction to continuous research for portable sensors [Chu *et al.*, 2010a; Myers *et al.*, 2013].

Recently, AlGa<sub>N</sub>/Ga<sub>N</sub> High Electron Mobility Transistors (HEMT) based sensors have made great attraction due to its excellent properties like wide bandgap, high mobility, chemical, and electrical stability in ionic medium and presence of surface charges to realize high sensitivity and fast response time [Makowski *et al.*, 2013; Nigam *et al.*, 2017]. The HEMTs are “normally on” due to the availability of two-dimensional electron gas (2DEG) at the heterointerface of AlGa<sub>N</sub> and Ga<sub>N</sub>, which provides a conducting channel without applying any gate voltage. Thus, it eliminates the requirement of a reference electrode, reduces the complexity of the sensor [Nigam *et al.*, 2019b]. Using these excellent properties, the AlGa<sub>N</sub>/Ga<sub>N</sub> HEMTs were used in different ion sensing applications without employing any reference electrode [Myers *et al.*, 2013; Nigam *et al.*, 2019b; Wang *et al.*, 2007].

The 2,5-di-mercapto-1,3,4-thiadiazole (DMTD) is a fascinating ligand and has been used for low-level determination of Pb<sup>2+</sup> ions by spectrofluorimetric, photometric, electrochemical approaches [Jamaluddin Ahmed and Mamun, 2001; Vasimalai and John, 2011; Wu *et al.*, 2008]. The structural, chemical, and optical properties of DMTD have been extensively studied in various reports [Maiti *et al.*, 2016; Matsumoto *et al.*, 1999; Tatsuma *et al.*, 1997; Vasimalai and John, 2011]. It has five donor atoms in deprotonated and protonated forms. These donor atoms can form mono and multinuclear complexes with metals. Moreover, DMTD occurs as a thiolate form in the solid-state, whereas it occurs in three forms, namely, dithiol, thiolate, and dithione in solution. Depending upon the reaction with metal ions, DMTD can coordinate with both the thiocarbonyl sulfur atoms, or both the nitrogen atoms, or one sulfur atom, and one nitrogen atom. The DMTD can also coordinate with the metal ions using the electrons in the aromatic heterocyclic ring [Maiti *et al.*, 2016; Vasimalai and John, 2011].

## 6.2 CHEMICAL USED IN THE EXPERIMENT

The materials used for this experimental work are 2,5-di-mercapto-1,3,4-thiadiazole (DMTD), purchased from Sigma-Aldrich. HPLC Water, Sodium Hydroxide (NaOH), Lead (II) nitrate, Copper (II) sulfate, Chromium (III) nitrate, Cadmium (II) nitrate, Nickel (II) nitrate, zinc (II) nitrate were purchased from Merck. The solutions of different concentrations of Pb<sup>2+</sup> ions were prepared in ammonium acetate buffer. The pH was adjusted by adding HNO<sub>3</sub> or NaOH solutions. Other reagents used here were of analytical grade [Nigam *et al.*, 2019b].

## 6.3 DMTD FUNCTIONALIZATION ON THE GATE REGION OF AlGa<sub>N</sub>/Ga<sub>N</sub> HEMT

The functionalization process of the DMTD on the gate region of HEMT is shown in Figure 6.1. The 1 mM DMTD solution was prepared in 15 ml ethanol in which the AlGa<sub>N</sub>/Ga<sub>N</sub> HEMT was soaked for 12 hrs. at room temperature. The modified gate region was rinsed with fresh ethanol and deionized (DI) water to remove additional physisorbed molecules. The DMTD has a thiol group which consists of Sulfur (S). When the DMTD was functionalized on the active gate region, Au–S bond formed between the Au and DMTD, as shown in Figure 6.1. The Au–S bond was also confirmed by X-ray Photoemission Spectroscopy (XPS) [Wang *et al.*, 2007]. Additionally,

Raman analysis further confirms the bonding between DMTD and Au [Kalimuthu *et al.*, 2009], and hence, the DMTD was functionalized on Au gated AlGa<sub>N</sub>/Ga<sub>N</sub> HEMT.

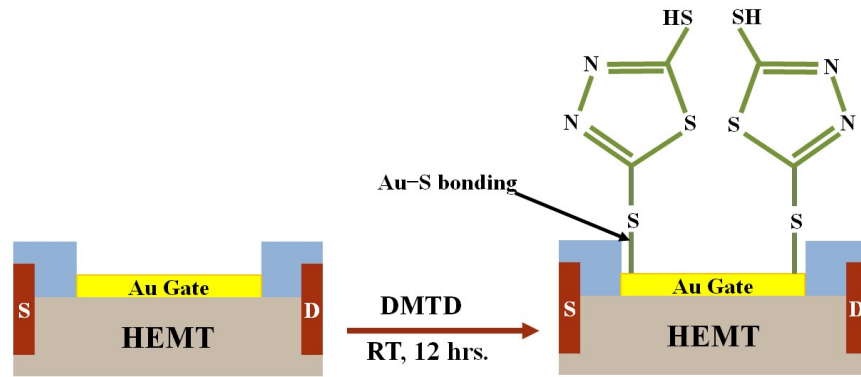


**Figure 6.1:** Functionalization of DMTD on the gate region of AlGa<sub>N</sub>/Ga<sub>N</sub> HEMT.

#### 6.4 MEASUREMENT AND CHARACTERIZATION

The electrical characterization of the developed sensor was carried out using the Keithley-4200 semiconductor characterization system (SCS) similarly described in chapter 5. Here, the source and drain contacts were utilized for measurement while the gate region was remained open for liquid exposure. When the gate terminal of the HEMT was exposed to different concentrations of Pb<sup>2+</sup> ions, the variation in the drain to source current ( $I_{DS}$ ) was observed for the fixed drain to source voltage ( $V_{DS}$ ). The solutions prepared with the different Pb<sup>2+</sup> ion concentrations ranging from 0.01 ppb to 1 ppm in 50 mM ammonium acetate buffer [Nigam *et al.*, 2019b].

#### 6.5 ELECTRICAL RESPONSE OF DMTD FUNCTIONALIZED AlGa<sub>N</sub>/ Ga<sub>N</sub> HEMT SENSOR FOR Pb<sup>2+</sup> IONS

The electrical response of the developed sensor with different concentrations from Pb<sup>2+</sup> ion free buffer solution (blank solution) to 10 ppm Pb<sup>2+</sup> ion solution is shown in Figure 6.2. When the Pb<sup>2+</sup> ions interact with the DMTD functionalized Au gated AlGa<sub>N</sub>/Ga<sub>N</sub> HEMT at the fixed drain to source voltage ( $V_{DS}$ ) of +0.5 V, the variation in the drain to source current ( $I_{DS}$ ) was measured. Interestingly, the  $I_{DS}$  did not change when the blank solution interacts with the gate region of the device. However, an increment in the  $I_{DS}$  was observed for 10 ppt (parts per trillion) Pb<sup>2+</sup> ion solution.

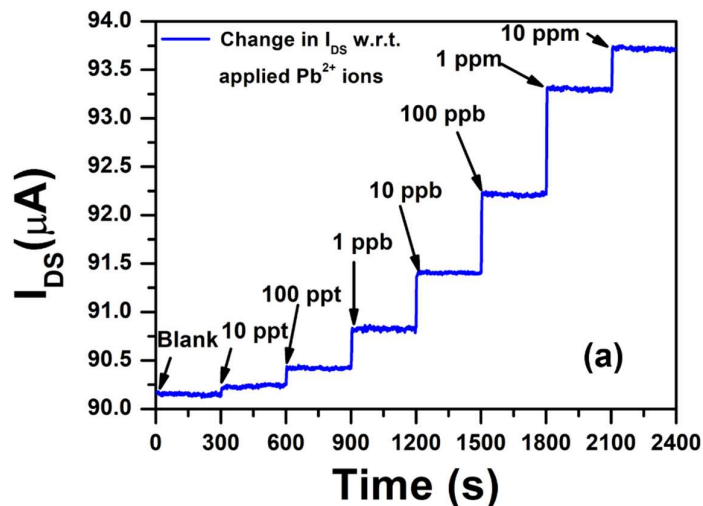


**Figure 6.2:** Real-time response of AlGa<sub>N</sub>/ Ga<sub>N</sub> HEMT sensor for Pb<sup>2+</sup> ion concentrations ranging from blank solution to 10 ppm concentration ( $V_{DS} = +0.5$  V)

The results showed the increment in the  $I_{DS}$  with the increase in the concentration of  $Pb^{2+}$  ions. It was appeared due to the captured  $Pb^{2+}$  ions that form the Pb-DMTD complex. This process increases the conductivity of the 2DEG channel, and therefore the  $I_{DS}$  changed at fixed  $V_{DS}$ . It can be observed from Figure 6.2 that the enhancement in  $I_{DS}$  is small for 10 ppm as compared to 1 ppm indicates that  $I_{DS}$  starts saturating at a higher concentration of  $Pb^{2+}$  ions [Nigam *et al.*, 2019b]. The electrical response of the sensor was observed at each concentration for 300 seconds.

## 6.6 LIMIT OF DETECTION, RESPONSE TIME, AND SENSITIVITY ANALYSIS

The calibration plot for  $I_{DS}$  vs.  $Pb^{2+}$  ion concentration in the range of 0.01 ppb – 1000 ppb is displayed in Figure 6.3. The plot for lower concentration is shown in the inset of Figure 6.3. The limit of detection (LoD) and sensitivity of the sensor can be calculated by a similar process (standard 3 sigma approach) followed in chapter 5. By the calibration curve, the sensitivity of the  $Pb^{2+}$  ion sensor (slope of calibration curve) was determined as  $0.607 \mu A/ppb$ . Other parameters such as  $\sigma$  (standard deviation) and correlation coefficient ( $R^2$ ) was derived as 0.003725 and 0.9961, respectively. Thus, the LoD was obtained as 0.01841 ppb or 18.41 ppt, which is well below the standard limits of WHO and EPA for  $Pb^{2+}$  ions in drinking water [Nigam *et al.*, 2019b]. The response time of the sensor was also calculated by a similar process as explained in chapter 5 and observed that the sensor showed a rapid response time approximately 4 s at 10 ppt concentration [Nigam *et al.*, 2019b].

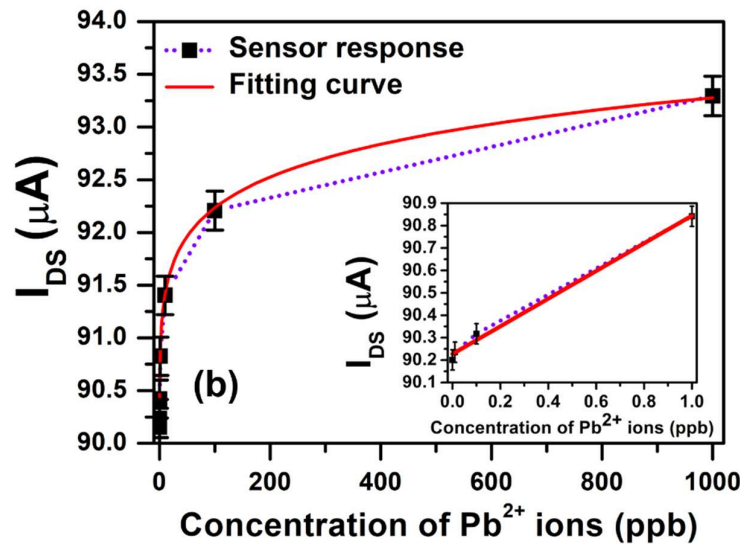


**Figure 6.3:** Calibration (fitting) curve and the sensor's response versus applied  $Pb^{2+}$  ion concentration (inset: response at a lower concentration).

## 6.7 SELECTIVITY ANALYSIS

The selectivity of the sensor was observed by utilizing the fixed interference method to calculate the amperometric selectivity coefficient [Maccà and Wang, 1995]. The sensor's response was observed by fixing the ion concentration of each interfering metal ions such as  $Hg^{2+}$ ,  $Ni^{2+}$ ,  $Cu^{2+}$ ,  $Zn^{2+}$ ,  $Cd^{2+}$ , and  $Cr^{3+}$  at 10 ppm and varying the concentration of  $Pb^{2+}$  ions (analyte) from 0.01 ppb to 10,000 ppb. Initially, the response was observed in the solution of interferent at 10 ppm. In this interferent solution, the 0.01 ppb concentration of  $Pb^{2+}$  was mixed and varied up to 10 ppm, and the total current response ( $I_{DS}(Pb^{2+}, j)$ ) was measured [Nigam *et al.*, 2019b]. Thus, the selectivity coefficient was calculated as:

$$k_{Pb^{2+},j}^{amp} = \frac{I_j}{C_j \cdot S} \quad (6.1)$$

where  $S$  is the slope of the calibration curve,  $j$  is interfering metal ions, and  $C_j$  is the concentration of interferent (here 10 ppm) [Maccà and Wang, 1995]. The calculated values of selectivity coefficient by Eq. (6.1) for interferents such as  $Hg^{2+}$ ,  $Cd^{2+}$ ,  $Cu^{2+}$ ,  $Cr^{3+}$ ,  $Ni^{2+}$ , and  $Zn^{2+}$  with  $Pb^{2+}$  ions are  $2.14 \times 10^{-2}$ ,  $1.14 \times 10^{-2}$ ,  $1.56 \times 10^{-2}$ ,  $9.95 \times 10^{-3}$ ,  $1.012 \times 10^{-2}$ , and  $1.067 \times 10^{-2}$  respectively [Nigam *et al.*, 2019b]. It indicates that the proposed sensor is highly selective for  $Pb^{2+}$  ions.

### 6.8 IMPACT OF pH ON THE SENSING RESPONSE OF THE SENSOR

The effects of pH on the sensing for the detection of  $Pb^{2+}$  ions were also observed, as shown in Figure 6.4. We examined  $I_{DS}$  of the HEMT sensor at 1 ppm concentration of  $Pb^{2+}$  ions prepared in acetate buffer solutions in the pH range of 3.0-9.0 to optimize the best pH conditions for the detection of  $Pb^{2+}$  ions. Initially, the  $I_{DS}$  increased by increasing pH from 3.0 to 5.0 and reached the maximum value of  $I_{DS}$  at pH 5.5. The  $I_{DS}$  starts decreasing by the continuous increment in pH.

The low response of the sensor at the lower pH (high acidic conditions) can be attributed to the nitrogen protonation of DMTD, and the ionization of the mercapto group in DMTD is also difficult at low pH. Whereas at high pH values, the reduction in  $I_{DS}$  can be due to the hydrolysis of  $Pb^{2+}$  ions [Wu *et al.*, 2008]. Hence acetate buffer solution of pH 5.5 provides a favorable condition for sensing of  $Pb^{2+}$  ions on DMTD functionalized AlGaIn/GaN HEMT sensor, and it has been used for all the experimental solutions. The reports on electrochemical (voltammetry) and spectrometric experiments for the detection of  $Pb^{2+}$  ions on DMTD also confirm that the highest sensitivity of  $Pb^{2+}$  ions was achieved around pH 5.5 [Vasimalai and John, 2011; Wu *et al.*, 2008].

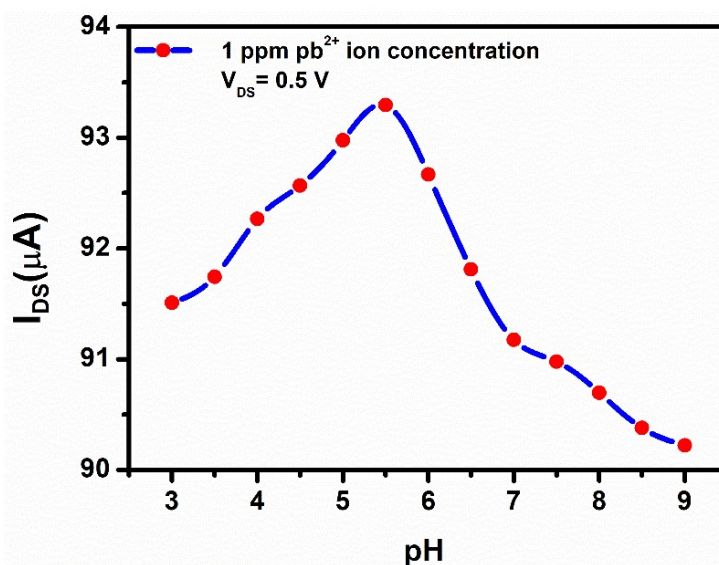


Figure 6.4: Effects of pH on  $I_{DS}$  of the sensor in 1 ppm concentration of  $Pb^{2+}$  ions.

### 6.9 DETECTION OF $Pb^{2+}$ IONS IN REAL WATER SAMPLES

The proposed sensor was also tested on real water samples. Here, the sensor was used to test tap water of the Indian Institute of Technology, Jodhpur, India, lake water (Kaylana lake in Jodhpur, India), and an as-prepared standard sample of 10 ppb  $Pb^{2+}$  ion concentration. The inductively coupled plasma mass spectroscopy (ICP-MS) was used as a reference method to observe the concentration of the samples for cross-correlation. Table 6.1 shows the detection of  $Pb^{2+}$  ions on real water samples by the proposed sensor, and the ICP-MS approach indicates that the sensor shows good agreement with the ICP-MS method.

**Table 6.1:** Detection of Pb<sup>2+</sup> Ions in Real Water Samples

Samples	Pb <sup>2+</sup> ion concentration (ppb)		
	Added	Observed by proposed sensor	Observed by ICP-MS
Standard	10	10	10.387
Tap water	0	1	0.93
Lake water	0	2	2.056

### 6.10 RECOVERY AND REPEATABILITY OF THE AlGa<sub>n</sub>/GAN HEMT SENSOR

The recovery of the HEMT sensor ions was performed by utilizing ammonium acetate buffer at pH 5.5 on the device for 50 s [Wu *et al.*, 2008]. Interestingly, the sensor response was recovered 99.73% by this process. Figure 6.5 showed the response and recovery of the HEMT sensor for Pb<sup>2+</sup> ions. The optimization process of recovery time was carried out by a similar process followed in our previous report [Nigam *et al.*, 2019b]. Moreover, the repeatability of the sensor was observed by performing the sensing operation under the same operating conditions. It is evident from Figure 6.6 that the variation in the response was trivial, which indicates the excellent repeatability of the sensor.

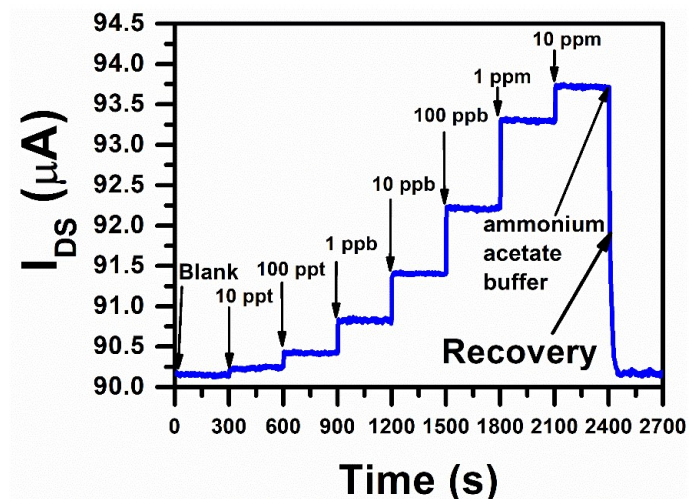


**Figure 6.5:** Response and recovery of Pb<sup>2+</sup> ion AlGa<sub>n</sub>/ GaN HEMT sensor

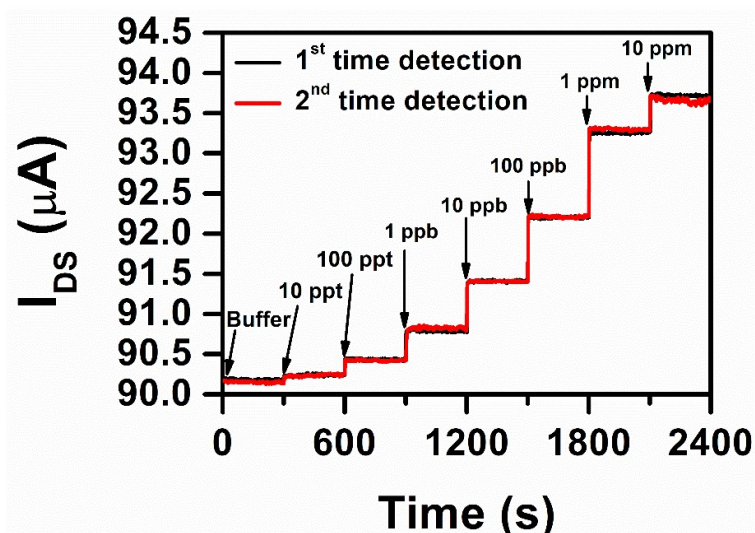


**Figure 6.6:** Repeatability analysis of the sensor

## 6.11 COMPARATIVE ANALYSIS OF THE DEVELOPED Pb<sup>2+</sup> ION SENSOR WITH OTHER METHODOLOGIES

The result obtained in the present work for Pb<sup>2+</sup> ion detection on DMTD functionalized AlGa<sub>0.5</sub>N/GaN HEMT is compared with the previously reported sensors based on different methods and are shown in Table 6.2. It can be observed from Table 6.2 that the present sensor showed a rapid response for the detection of Pb<sup>2+</sup> ions as compared to other methods that have the response time more than a few minutes. The proposed sensor also is shown the limit of detection (LoD) of 0.018 ppb or 18 ppt, which is very low compared to other sensors. Additionally, the sensitivity of the sensor also compared with other processes and found the sensor is highly sensitive for the detection of Pb<sup>2+</sup> ions.

**Table 6.2 :** Comparison of The Proposed Sensor with other Lead Ion Sensors

Functionalizing material	Analyte (ions)	Process	Sensitivity ( $\mu\text{A/ppb}$ )	LoD (ppb)	Response time or Accumulation time	References
DMTD	Pb <sup>2+</sup>	Functionalization on AlGa <sub>0.5</sub> N/GaN HEMT	0.607	0.018	~ 4 seconds	This work
DMTD	Pb <sup>2+</sup>	Stripping voltammetry	—	20.7	—	[Vasimalai and John, 2011; Wu <i>et al.</i> , 2008]
DMTD	Pb <sup>2+</sup>	Spectrophotometry	—	0.5	4 min.	[Jamaluddin Ahmed and Mamun, 2001; Vasimalai and John, 2011]
ion-selective membrane	Pb <sup>2+</sup>	Functionalization on AlGa <sub>0.5</sub> N/GaN HEMT	—	0.0207	10-15 min.	[Chen <i>et al.</i> , 2018]
GSH-AuNp	Pb <sup>2+</sup>	Colorimetry	—	20.7	15-20 min.	[Chai <i>et al.</i> , 2010]
Cu/Nafion/Bi	Pb <sup>2+</sup>	Differential Pulse Voltammetry	0.2031	0.62	300 sec.	[Legeai and Vittori, 2006]
Screen-printed electrode	Pb <sup>2+</sup>	square wave anodic stripping voltammetry	0.176 $\pm$ 0.085	1.8	—	[Güell <i>et al.</i> , 2008]
Bi/Edge plane pyroelectric graphite	Pb <sup>2+</sup>	Anodic stripping voltammetry	0.0354	0.084	240 sec.	[Kachoosangi <i>et al.</i> , 2007]
Ion Imprinted polymer	PO <sub>4</sub> <sup>3-</sup>	Functionalization on AlGa <sub>0.5</sub> N/GaN HEMT	0.003191	1.97	—	[Jia <i>et al.</i> , 2016]
Thioglycolic acid	Hg <sup>2+</sup>	Functionalization on AlGa <sub>0.5</sub> N/GaN HEMT	—	27	<5 seconds	[Wang <i>et al.</i> , 2007]

## 6.12 SENSING MECHANISM OF THE DETECTION OF Pb<sup>2+</sup> IONS USING DMTD FUNCTIONALIZED AlGa<sub>0.5</sub>N/GaN HEMT SENSOR

The possible mechanism of the proposed DMTD functionalized AlGa<sub>0.5</sub>N/GaN HEMT sensor for Pb<sup>2+</sup> ion detection is explained in Figure 6.7. DMTD was functionalized on the Au-gated AlGa<sub>0.5</sub>N/GaN HEMT by the Au-S bonding. The DMTD contains -SH group, which could bind with Pb<sup>2+</sup> ions to make the Pb-DMTD complex. The stoichiometric composition of the complex is 1:2 for Pb and DMTD, respectively [Vasimalai and John, 2011; Wu *et al.*, 2008]. This

metal-organic complex acquires net positive charges, which in turn raises the gate potential and hence, escalate the electron density ( $n_s$ ) of the 2DEG of the AlGa<sub>x</sub>N/GaN HEMT as follows [Jia *et al.*, 2016; Nigam *et al.*, 2019b]:

$$n_s = \frac{\epsilon_n}{qd} (V_G - V_T - V(x)) \quad (6.2)$$

where  $q$  is the electron charge,  $V_G$  is gate potential,  $\epsilon_n$  is the total permittivity of AlN spacer layer, Al<sub>x</sub>Ga<sub>1-x</sub>N barrier layer, and GaN cap layer;  $d$  is the distance between the device surface and 2DEG,  $V_T$  is the threshold voltage, and  $V(x)$  is channel potential of the device. As  $n_s$  changes, mobility also changes as scattering processes increase or decrease. The increment in the electron density ( $n_s$ ) increases the  $I_{DS}$  of the device [Charfeddine *et al.*, 2012]. The variation of the  $I_{DS}$  for change in gate potential after exposure to Pb<sup>2+</sup> ions can also be given as [Nigam *et al.*, 2019b]:

$$I_{DS} = \frac{\epsilon_n \mu W}{2dL} [2(V_G - V_T)V_{DS} - V_{DS}^2] \quad (6.3)$$

where  $\mu$  is the electron mobility in 2DEG,  $W$ , and  $L$  are the channel width and channel length, respectively. Thus, this scheme of electrical characterization enables the measurement of variations in 2DEG and  $I_{DS}$  by changes in the gate potential appearing from the application of different Pb<sup>2+</sup> ion concentrations on the DMTD functionalized gate region.

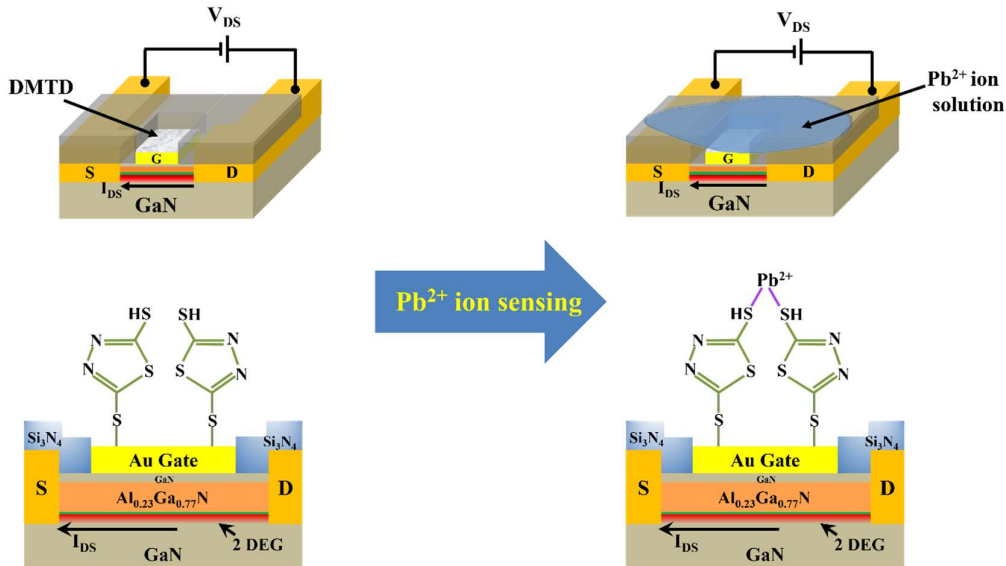


**Figure 6.7:** Proposed mechanism of DMTD functionalized AlGa<sub>x</sub>N/GaN HEMT sensor for Pb<sup>2+</sup> ion detection.

### 6.13 CONCLUSION

In this chapter, a DMTD functionalized AlGa<sub>x</sub>N/GaN HEMT has been fabricated for the detection of toxic Pb<sup>2+</sup> ions. The Pb<sup>2+</sup> ions detection was performed by observing variation in  $I_{DS}$  after employing Pb<sup>2+</sup> ions on the gate region. The sensor exhibits a high sensitivity of 0.607  $\mu$ A/ppb and a rapid response time of  $\sim$  4 seconds, and a detection limit around 18.41 ppt, which is an extremely low concentration of Pb<sup>2+</sup> ions detected by the AlGa<sub>x</sub>N/GaN HEMT sensor. The sensor also showed highly selective behavior towards Pb<sup>2+</sup> ions. These results make the DMTD functionalized AlGa<sub>x</sub>N/GaN HEMT sensor a promising candidate for ultra-low-level detection of Pb<sup>2+</sup> ions.

...